Biochem. J. (1992) 284, 275–281 (Printed in Great Britain)

Kinetic resolution of the separate GLUT1 and GLUT4 glucose transport activities in 3T3-L1 cells

Robin W. PALFREYMAN,* Avril E. CLARK,* Richard M. DENTON,† Geoffrey D. HOLMAN* and Izabela J. KOZKA*

*Department of Biochemistry, University of Bath, Claverton Down, Bath BA2 7AY, U.K., and †Department of Biochemistry, University of Bristol, University Walk, Bristol BS8 1TD, U.K.

A bis-mannose-photolabel-displacement method has been developed for resolving the separate kinetic properties of the glucose transporters GLUT1 and GLUT4, which are both present in 3T3-L1 cells. We have quantified the cell-surface transporter abundance ($B_{max.}$) for the two isoforms by displacing radiolabelled 2-*N*-[4-(1-azi-2,2,2-trifluoroethyl)benzoyl]-1,3-bis-(D-mannos-4-yloxy)-2-propylamine (ATB-BMPA) by non-labelled ATB-BMPA. In cells acutely treated with insulin, the GLUT1 $B_{max.}$ was 0.19 μM and the GLUT4 $B_{max.}$ was 0.17 μM. In cells which were chronically treated with insulin, the GLUT1 $B_{max.}$ was increased by ~ 4-fold to 0.7 μM, whereas the GLUT4 was decreased by ~ 50% ($B_{max.}$ = 0.1 μM). However, this large increase in total concentrations of cell-surface transporters (the sum of GLUT1 and GLUT4 concentrations) was not reflected in a large increase in 3-*O*-methyl-D-glucose transport, suggesting that GLUT1 makes a smaller contribution to transport than does GLUT4. In acutely insulin-treated cells at 37 °C, the apparent kinetic parameters for 3-*O*-methyl-D-glucose transport were $V_{max.}^{app.}$ = 0.52 mM·s^{-1} and $K_m^{app.}$ = 12.3 mM. In chronically insulin-treated cells the $V_{max.}^{app.}$ = 1.24 mM·s^{-1} and $K_m^{app.}$ = 23.0 mM. We have measured the displacement of ATB-BMPA by different concentrations of 3-*O*-methyl-D-glucose to resolve the separate affinity constants of GLUT1 and GLUT4 for this transported ligand. In acute- and chronic-insulin-treated cells the GLUT1 K_m for 3-*O*-methyl-D-glucose was ~ 20 mM, and the GLUT4 K_m for 3-*O*-methyl-D-glucose was ~ 7 mM. An analysis of these data and the 3-*O*-methyl-D-glucose transport rates was carried out to calculate transport capacity (TK values) for the two isoforms at 37 °C. In acute- and chronic-insulin-treated cells the TK values were 0.36×10^4 mM^{-1}·min^{-1} for GLUT1 and 1.13×10^4 mM^{-1}·min^{-1} for GLUT4. Thus GLUT1 has an ~ 3-fold lower transport capacity than GLUT4 at low concentrations of transported sugar. The lower GLUT1 transport capacity was shown to be mainly due to the high K_m of GLUT1. The calculated turnover numbers were 7.2×10^4 min^{-1} for GLUT1 and 7.9×10^4 min^{-1} for GLUT4.

INTRODUCTION

Five major mammalian glucose transporter isoforms appear to show some markedly specific tissue distributions. It has been suggested [1–3] that the abundance of a distinct isoform in a particular tissue is related to its transport kinetic properties and therefore its function in that tissue. Cultured cells have been shown to contain high concentrations of the GLUT1 isoform. Cell transformation with oncogenes [4,5], growth factors [6,7], cytokines [8,9] and starvation [10–12] have been shown to increase markedly the concentration of this transporter, with a consequent increase in glucose transport activity. It has been proposed that GLUT2 has a high K_m for D-glucose so that it can function to export rapidly a large range of glucose concentrations from a liver which is undergoing rapid glycogenolysis [13]. The GLUT3 isoform has been detected in many cell and tissue types, including brain and foetal muscle [14]. The GLUT4 isoform has a relatively low K_m, and the translocation of this isoform to the cell surface of adipose cells and muscle [15–19] is stimulated by insulin. The GLUT5 isoform is found in intestinal enterocytes and kidney [20]. Tissue specialized metabolic requirements and kinetic demands for glucose can thus be regulated by expression of tissue-specific transporter isoforms which have distinct transport kinetic properties.

Cultured 3T3-L1 cells also contain high levels of the GLUT1 isoform, but can be differentiated in a regime involving insulin, dexamethasone and isobutylmethylxanthine treatment to give high levels of the acutely insulin-sensitive isoform GLUT4. Calderhead *et al.* [21] and Kozka *et al.* [12] have shown that the acute insulin treatment increases the cell-surface availability of both GLUT4 and GLUT1, so that both are present at the surface in equal amounts. Tordjman *et al.* [22] and Kozka *et al.* [12] have shown, however, that a 24 h chronic insulin treatment increases GLUT1 by 4–5-fold. We have shown [12], by cell-surface labelling, that GLUT4 is down-regulated by 50%. Thus there is a marked change in the isoform type (the GLUT1 : GLUT4 ratio increases to 10:1) and a large change in the total concentration of transporter, but these changes are associated with an only ~ 40% increase in transport activity, as measured by the uptake of 2-deoxy-D-glucose at tracer concentrations. These findings suggest that GLUT4 and GLUT1 make unequal contributions to the transport rate. To analyse this possibility further, a method for resolving the separate parameters of GLUT1 and GLUT4 kinetic contributions to transport activity is thus required.

Further analysis of the kinetic differences between the GLUT1 and GLUT4 isoforms that are present in 3T3-L1 cells has necessitated the use of the non-metabolized analogue 3-*O*-methyl-D-glucose in transport kinetic measurements. Because transport measurements alone cannot be easily used to calculate K_m and $V_{max.}$ for each transporter (four parameters), we have determined the separate affinities of the two isoforms for 3-*O*-methyl-D-glucose by measuring the displacement of the bis-mannose photolabel 2-*N*-[4-(1-azi-2,2,2-trifluoroethyl)benzoyl]-1,3-bis-(D-mannos-4-yloxy)-2-propylamine (ATB-BMPA) by a range of concentrations of 3-*O*-methyl-D-glucose. By measuring the binding of the photolabel at a range of ATB-BMPA concentrations,

Abbreviations used: ATB-BMPA, 2-*N*-[4-(1-azi-2,2,2-trifluoroethyl)benzoyl]-1,3-bis-(D-mannos-4-yloxy)-2-propylamine; DMEM, Dulbecco's modified Eagle's medium; $C_{12}E_9$, nona(ethylene glycol) dodecyl ether.

we have determined the concentrations of GLUT1 and GLUT4 at the cell surface. We show how the use of data on transporter concentration and affinity for 3-*O*-methyl-D-glucose can be used to simplify the analysis of transport data to resolve just two parameters (the TK values for GLUT1 and GLUT4). Since the TK is the turnover number divided by K_m (or $V_{max.}/K_m$ divided by transporter concentration), we have used this parameter to calculate the transporter turnover number for each isoform. The TK is formally equivalent to an association constant [23,24]. The TK thus represents the maximum permeability (or transport capacity) of each transporter. A low transporter capacity (TK) is thus due to a low association with substrate because of either a low turnover or a low affinity. We have also examined the issue of photolabelling efficiency.

MATERIALS AND METHODS

Materials

ATB-BMPA and ATB-[2-^{3}H]BMPA (sp. radioactivity ~ 10 Ci/mmol) were prepared as described previously [25,26]. 3-*O*-Methyl-D-[U-^{14}C]glucose was from Amersham International. Dulbecco's modified Eagle's medium (DMEM) was from Flow Laboratories. Foetal-bovine serum was from Gibco. Monocomponent pig insulin was a gift from Dr. Ronald Chance, Eli Lilly Corp. Dexamethasone, isobutylmethylxanthine, phloretin, 3-*O*-methyl-D-glucose and Protein A–Sepharose were from Sigma. $C_{12}E_9$ [nona(ethylene glycol) dodecyl ether] was from Boehringer.

Cell culture

3T3-L1 fibroblasts were obtained from American Type Culture Collection and were cultured in DMEM and differentiated to adipocytes by treatment with insulin, dexamethasone and isobutylmethylxanthine as described previously [12,21,27]. Before use in 3-*O*-methyl-D-glucose transport assays or in cell-surface labelling experiments, the cells were subjected to a standard washing procedure. Cells were washed with phosphate-buffered saline (154 mM-NaCl, 12.5 mM-sodium phosphate, pH 7.4) and were then incubated for 2 h in serum-free medium containing 25 mM-D-glucose. This was followed by three washes in Krebs–Ringer–Hepes (KRH) buffer (136 mM-NaCl, 4.7 mM-KCl, 1.25 mM-$CaCl_2$, 1.25 mM-$MgSO_4$, 10 mM-Hepes, pH 7.4). Cells were then maintained at 37 °C with or without 100 nM pig monocomponent insulin for 30 min in 1 ml of KRH buffer. In chronic-insulin treatment, fully differentiated cells were incubated for 24 h in DMEM with 25 mM-glucose and 500 nM insulin.

3-*O*-Methyl-D-glucose transport assays

3T3-L1 cell monolayers in 35 mm-diam. dishes, treated as described above, were equilibrated with 0–40 mM-3-*O*-methyl-D-glucose in 0.5 ml of KRH buffer for 30 min at 37 °C. The cells were then incubated with 0.5 ml of KRH containing the equilibrium concentrations of 3-*O*-methyl-D-glucose and 0.3 μCi of 3-*O*-methyl-D-[U-^{14}C]glucose. At 10 s for insulin-treated cells and at 120–160 s for basal cells, 1 ml of ice-cold KRH containing 0.3 mM-phloretin was added to arrest transport. The dishes were rapidly washed three times in the stopping solution. The cell-associated radioactivity was then extracted and counted. The radioactivity associated with the cells at zero time was determined by adding stopping solution before the radioactive 3-*O*-methyl-D-glucose. The radioactivity associated with the cells at equilibrium was determined by incubating insulin-treated cells with 3-*O*-methyl-D-glucose for 15 min. The total cell volume per 35 mm dish was calculated from the equilibrated 3-*O*-methyl-D-glucose and was found to be 2.81 ± 0.43 μl/dish (from six experiments; two experiments acute-insulin, three experiments chronic-insulin, one experiment basal). Equilibrium exchange uptake rate constants (k) were then calculated from the equation $k = n(1-f)/t$, where t is the uptake time and f is the fractional filling [28,29]. In experiments used to estimate the half-maximal inhibition constant (K_i) for ATP-BMPA, the inhibitor was added with 50 μM-3-*O*-methyl-D-glucose as substrate. The extent of irreversible inhibition of transport produced by photoincorporation of ATB-BMPA was determined by irradiating cells in 35 mm dishes (for 1 min in a Rayonet photochemical reactor [12]) in the presence of 0.5–2 mM-ATB-BMPA in 500 μl of KRH. The dishes were then washed three times in KRH to remove non-incorporated ATB-BMPA and then assayed for residual transport of 50 μM-3-*O*-methyl-D-glucose as described above.

ATB-BMPA photolabelling

Differentiated cells in 35 mm dishes were washed in KRH buffer at 37 °C and were irradiated for 1 min in the presence of 100 μCi of ATB-[2-^{3}H]BMPA as described previously [12]. To determine the binding kinetic parameters, the specific radioactivity of the label was decreased by addition of non-radioactive ATB-BMPA at the concentrations indicated in the Figures. Bound ATB-BMPA (mol) was calculated from the d.p.m. recovered after immunoprecipitation and gel electrophoresis of the photolabelled GLUT1 or GLUT4. The free ATB-BMPA was assumed to be equal to the combined concentration of the non-radioactive and radioactive ligand, and was not corrected for the small amount of ATB-BMPA bound to the cells.

Immunoprecipitation and electrophoresis

The irradiated cells were washed three times in KRH buffer and solubilized in 1.5 ml of detergent buffer, containing 2% $C_{12}E_9$, 5 mM-sodium phosphate and 5 mM EDTA, pH 7.2, and with the proteinase inhibitors antipain, aprotinin, pepstatin and leupeptin, each at 1 μg/ml. After centrifugation at 20000 $g_{max.}$ for 20 min, the supernatants were subjected to sequential immunoprecipitation with 20 μl of Protein A–Sepharose coupled to 100 μl of either anti-GLUT1 or anti-GLUT4 antiserum. These antisera were raised against *C*-terminal peptides as described previously [23,26]. After incubation for 1.5–2 h at 0–4 °C and washing of the immunoprecipitates three times with 1.0% and once with 0.1% $C_{12}E_9$ detergent buffer, the labelled glucose transporters were released from the antibody complexes with electrophoresis sample buffer (10% SDS/6 M-urea/10% mercaptoethanol) and then subjected to electrophoresis on 10%-acrylamide gels. The radioactivity on the gel was measured by cutting and counting gel slices. The radioactivity in transporter peaks was corrected for a background which was based on the average radioactivity of the slices on either side of the peak [21]. We have determined that, after immunoprecipitation with anti-GLUT1 and anti-GLUT4 antibodies, the amount of photolabelled transporter remaining in the supernatants is < 20% of the unprecipitated total of labelled transporters.

RESULTS

3-*O*-Methyl-D-glucose transport

The exchange uptake of 3-*O*-methyl-D-glucose was studied. This transport protocol was equivalent to that used in the photolabel-displacement experiments described below. Thus the cells were pre-equilibrated with non-radioactive 3-*O*-methyl-D-glucose, and then the influx of radioactive 3-*O*-methyl-D-glucose was measured. When a single transporter isoform is present, the concentration of 3-*O*-methyl-D-glucose at which the rate constant is decreased by half is formally equivalent to the equilibrium binding constant between 3-*O*-methyl-D-glucose and the trans-

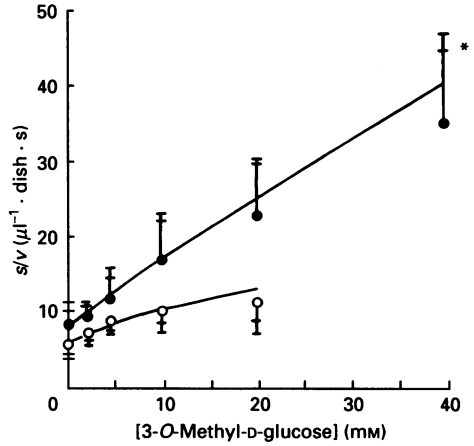

Fig. 1. Equilibrium exchange uptake of 3-*O*-methyl-D-glucose in 3T3-L1 cells

3T3-L1 cells in 35 mm dishes were either acutely treated with 100 nM-insulin for 30 min (●) or chronically treated with 500 nM-insulin for 24 h (○), and uptake of 3-*O*-methyl-D-glucose was determined as described in the Materials and methods section. s/v, the reciprocal of the uptake rate constant, was plotted against the 3-*O*-methyl-D-glucose concentration. The values shown were means from four experiments each with triplicate estimates of uptake rate constants. The inner S.E.M. bars were calculated with $n = 12$ (combining the replicate values), and the outer S.E.M. bars were calculated with $n = 4$ (by using the mean of the replicates from each independent experiment), except the value indicated by *, where the inner bar is the S.E.M. ($n = 4$) and the outer bar is the S.E.M. ($n = 12$). To convert the s/v values from $\mu l^{-1} \cdot$dish$\cdot$s into s, the plotted values were divided by the equilibrium intracellular volume of 2.81 μl/dish. The lines for both acute and chronic insulin treatments were derived from a single set of calculated TK values of 3.58×10^3 and 11.34×10^3 mM$^{-1} \cdot$min^{-1} for GLUT1 and GLUT4 respectively and by using the $B_{max.}$ and K_m values listed in row 5 of Table 1.

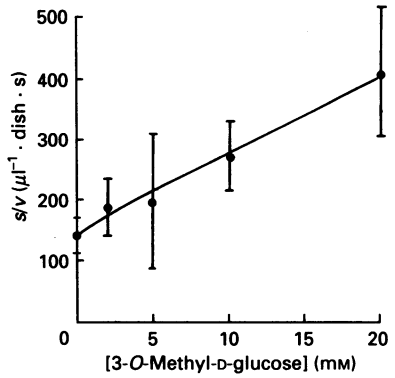

Fig. 2. Equilibrium exchange uptake of 3-*O*-methyl-D-glucose in basal 3T3-L1 cells

The uptake of 3-*O*-methyl-D-glucose into basal cells was determined as described in the Materials and methods section. s/v, the reciprocal of the uptake rate constant (●), was plotted against 3-*O*-methyl-D-glucose concentration, and the values are means ± S.E.M. ($n = 6$ from two experiments with triplicate estimates of the uptake rate constants). Additional experiments were carried out at 50 μM-3-*O*-methyl-D-glucose to estimate the range of variation of basal activity between experiments. In basal cells the s/v value was 144.9 ± 18.1 $\mu l^{-1} \cdot$dish$\cdot$s ($n = 11$, mean ± S.E.M. of 11 experiments each with triplicate estimates of the rate constants). In this series of experiments, acute insulin treatment decreased the s/v value 15-fold, to 9.57 ± 1.64 $\mu l^{-1} \cdot$dish$\cdot$s ($n = 11$, mean ± S.E.M. from 11 experiments each with triplicate estimates of the rate constant). To convert the s/v values from $\mu l^{-1} \cdot$dish$\cdot$s into s, the plotted values were divided by the equilibrium intracellular volume of 2.81 μl/dish. The line was derived from the TK, $B_{max.}$ and K_m values listed in row 6 of Table 1.

porter (the equilibrium exchange K_m). This has been shown to equal the concentration of 3-*O*-methyl-D-glucose that displaces the binding of tracer concentrations of another ligand such as cytochalasin B or ATB-BMPA [30].

When two isoforms are present, the relationship between the reciprocal of the exchange rate constant and the 3-*O*-methyl-D-glucose concentration may be curvilinear. The reciprocal plots shown in Fig. 1 are slightly curved, and this is likely to be due to the varying contributions of the two isoforms as the 3-*O*-methyl-D-glucose concentration is varied. The lines in Fig. 1 were therefore derived from the analysis of the separate GLUT1 and GLUT4 contributions to transport as described in the Discussion section. Fitting the data to the Michaelis–Menten equation, however, revealed an apparent K_m for 3-*O*-methyl-D-glucose of 12.3 ± 1.3 mM and $V_{max.} = 0.52 \pm 0.04$ mM$\cdot$s^{-1} in acute-insulin-treated cells (derived from the mean values of the rate constants from four experiments). These estimates are similar to those determined by Clancy *et al.* [31], who have also measured the kinetic parameters for 3-*O*-methyl-D-glucose transport in insulin-stimulated 3T3-L1 cells. They report values of $K_m = 10.9$ mM and $V_{max.} = 2.76$ pmol/min per 10^6 cells. Calculations using their estimate of cell volume of 5.6 μl/10^6 cells gave a $V_{max.}$ of 0.46 mM$\cdot$s^{-1}. However, we note that the cell volume in our experiments was ~ 2–3-fold smaller than that estimated by Clancy *et al.* [31].

In chronically-insulin treated cells we have found that the apparent K_m and $V_{max.}$ were increased to 23.0 ± 9.1 mM and 1.24 ± 0.40 mM$\cdot$s^{-1} respectively (determined from mean values of the rate constants obtained from four experiments). The large S.E.M. for these parameters is due to the curvilinearity of the kinetic plot, rather than the between-experiment variations in the kinetic parameters. The chronic-insulin treatment altered the GLUT1:GLUT4 ratio from 1:1 to 10:1 (see below). Thus the high apparent K_m for 3-*O*-methyl-D-glucose transport found in this condition is likely to reflect a high GLUT1 K_m for this substrate.

The apparent K_m and $V_{max.}$ for 3-*O*-methyl-D-glucose transport in basal cells obtained by fitting of the Michaelis–Menten equation were 11.5 ± 1.7 mM and 0.028 ± 0.003 mM$\cdot$s^{-1} respectively (determined from mean values of the rate constants obtained in two experiments) (Fig. 2).

We have also determined the K_i for the bis-mannose photolabel, ATB-BMPA, as an inhibitor of 3-*O*-methyl-D-glucose uptake (Fig. 3). We have used a 3-*O*-methyl-D-glucose substrate concentration of 50 μM, which is low in comparison with the affinity of either GLUT1 or GLUT4 for 3-*O*-methyl-D-glucose. Under these conditions the K_i can be calculated from the equation $v_0/v = 1 + I/K_i$, where v_0/v is the fractional inhibition and I is the inhibitor concentration [29]. The calculated K_i was 263 ± 30 μM in the acute-insulin treatment, which was not significantly different from the K_i determined in chronically insulin-treated cells, which gave $K_i = 200 \pm 53$ μM (one experiment).

We have examined the efficiency of irreversible inactivation of the transport rate owing to photoincorporation of ATB-BMPA. We have found that, after irradiation of 3T3-L1 cells in the presence of 0.5 mM-, 1 mM- and 2 mM-ATB-BMPA and removal of unbound ligand by washing, 2-deoxy-D-glucose transport was inhibited by 48%, 54% and 68% respectively compared with untreated samples. Since at these concentrations of ATB-BMPA 33%, 20% and 12% of the sites are unoccupied (assuming a K_d for ATB-BMPA of 250 μM), it can be calculated that, when all the sites are occupied, ~ 75% of the sites would have been irreversibly inactivated (results from two experiments).

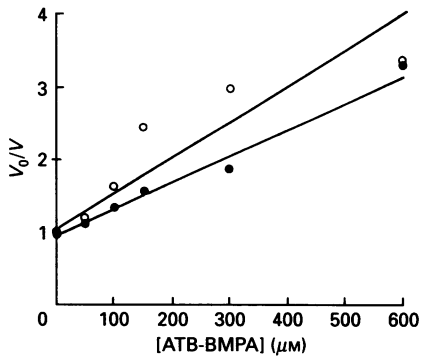

Fig. 3. Inhibition of 3-*O*-methyl-D-glucose uptake by ATB-BMPA

3T3-L1 cells in 35 mm dishes were either acutely (●) or chronically (○) treated with insulin, and the ratio of the rate constant for uptake of 50 μM-3-*O*-methyl-D-glucose in the absence and presence of ATB-BMPA (v_0/v) was plotted against the ATB-BMPA concentration (I). The results are from a single experiment with triplicate determinations of the rate constant. The line was derived by fitting the equation $v_0/v = 1 + I/K_i$ by using non-linear regression analysis weighted for relative error. This gave K_i values of 263 ± 30 μM (acute treatment) and 200 ± 53 μM (chronic treatment).

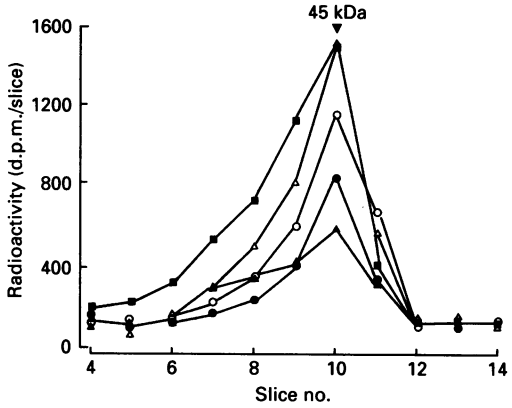

Fig. 4. Displacement of radiolabelled ATB-BMPA from GLUT4 by non-labelled ligand

3T3-L1 cells in 35 mm dishes were acutely treated with insulin and then photolabeled with 40 μM-ATB-[2-^{3}H]BMPA (100 μCi) either alone (■) or with additional non-labelled ATB-BMPA at 50 μM (△), 100 μM (○), 150 μM (●) or 300 μM (▲). GLUT4 was immunoprecipitated with anti-*C*-terminal-peptide antibody and subjected to electrophoresis. The radioactivity was measured by cutting and counting the gel slices. The data were used to calculate the concentration of ATB-BMPA bound. The position of the 45 kDa marker protein (ovalbumin) is shown

ATB-BMPA photolabelling

We have shown from results obtained by immunoprecipitating glucose transporters with antibodies against GLUT1 and GLUT4 *C*-terminal peptide that GLUT1 is the predominant isoform present in the cell membrane in the basal cells and that this is increased by ~ 3–5-fold after insulin treatment. Only low levels of GLUT4 were detected at the cell surface in the basal state, but an ~ 10–15-fold increase was observed after insulin treatment [12,21]. We have extended these observations here by measuring the binding of ATB-BMPA at a range of concentrations and calculated the K_d and apparent $B_{max.}$ for GLUT1 and GLUT4. Fig. 4 shows the displacement of ATB-[2-^{3}H]BMPA by a range of concentrations of non-labelled ATB-BMPA from GLUT4 in acutely insulin-treated cells. From these data the amount of ATB-BMPA bound was calculated, and these data were used to

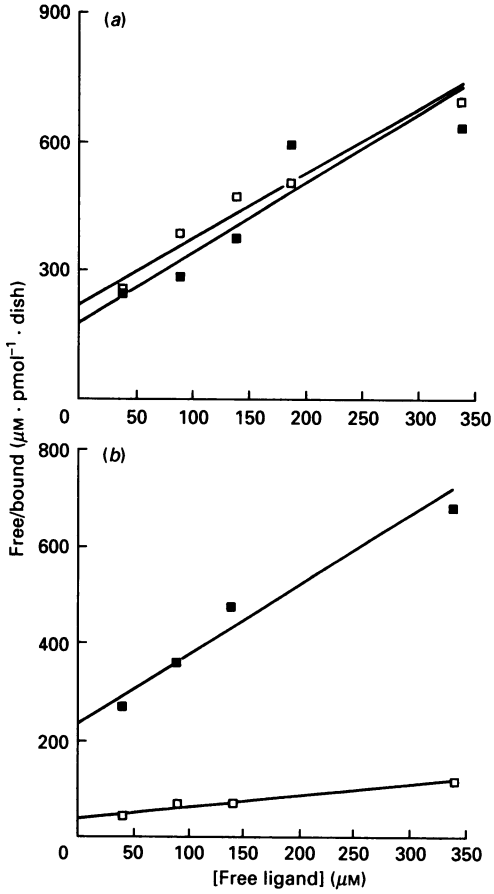

Fig. 5. Determination of the $B_{max.}$ values for ATB-BMPA binding to GLUT1 and GLUT4 glucose transporters in 3T3-L1 cells

3T3-L1 cells in 35 mm dishes were in (*a*) acutely treated with 100 nM-insulin for 30 min and in (*b*) chronically treated with 500 nM-insulin for 24 h and then described in the legend to Fig. 4, except that the data show the binding in immunoprecipitated GLUT4 (■) and GLUT1 (□). The results shown are from a single experiment. To convert the bound ATB-BMPA from pmol^{-1}·dish into μM, the values were divided by the equilibrium cell volume of 2.81 μl/dish. In acutely insulin-treated cells the GLUT1 $B_{max.}$ was 0.19 ± 0.03 μM and the GLUT4 $B_{max.}$ was 0.17 ± 0.03 μM (from three experiments). In chronically insulin-treated cells the GLUT1 $B_{max.}$ was 0.7 ± 0.07 μM, whereas the GLUT4 $B_{max.}$ was 0.099 ± 0.017 μM (from three experiments).

calculate $B_{max.}$ and K_d values by non-linear regression analysis of bound versus free ATB-BMPA concentration. Reciprocal plots are shown in Figs. 5(*a*) and 5(*b*). Fig. 5(*a*) shows that in acutely insulin-treated cells GLUT1 and GLUT4 have K_d values which were not significantly different and were ~ 150 μM. Thus binding of the photolabel at the high specific radioactivity of 10 Ci/mmol and low tracer concentrations of 40 μM (the present study) and 80 μM [12] is proportional to the number of GLUT1 and GLUT4 binding sites and is not dependent on an affinity difference between the two isoforms. We have previously shown that a chronic insulin treatment increases the tracer labelling of GLUT1 by 4–5-fold compared with the acute treatment. In Fig. 5(*b*) this is confirmed not to be due to an affinity change. The plots in Figs. 5(*a*) and 5(*b*) show bound ligand as pmol bound per 35 mm dish and are from one experiment. The $B_{max.}$ values were obtained from these data by dividing by the 3-*O*-methyl-D-glucose equilibrium space of 2.81 μl/dish, which gave transporter concentrations in μmol/l of intracellular water or μM. In acutely insulin-treated cells the GLUT1 $B_{max.}$ was 0.19 ± 0.03 μM and the GLUT4

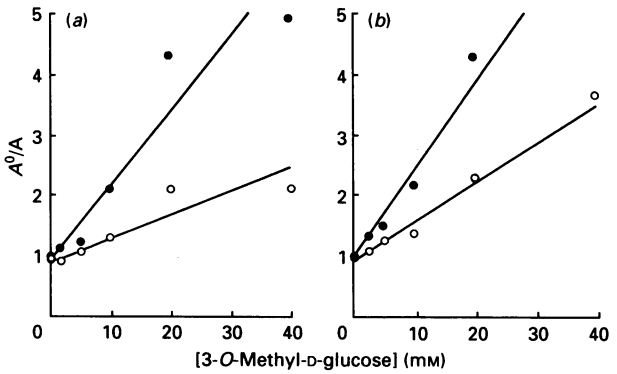

Fig. 6. Determination of the K_m values for 3-*O*-methyl-D-glucose displacement of ATB-BMPA from GLUT1 and GLUT4 glucose transporters in 3T3-L1 cells

3T3-L1 cells in 35 mm dishes were in (*a*) acutely treated with 100 nM-insulin for 30 min and in (*b*) chronically treated with 500 nM-insulin for 24 h and then photolabelled with 100 μCi of ATB-BMPA at the indicated concentrations of 3-*O*-methyl-D-glucose. Photolabelled GLUT1 (○) and GLUT4 (●) were then immunoprecipitated with anti-*C*-terminal-peptide antibodies and subjected to electrophoresis. Radioactivity was determined by cutting and counting gel slices. The ratio of the radioactivity associated with the peaks obtained in the absence (A^0) and presence (A) of competing ligand were then determined. The results shown are the mean values from three experiments (acute treatment) and two experiments (chronic treatment). The K_m values were obtained by fitting the equation $A^0/A = 1+s/K_m$ by using non-linear regression analysis weighted for relative error. In the acute treatment the GLUT1 K_m was 23.4±7.6 mM and the GLUT4 K_m was 7.2±2.0 mM. In the chronic treatment the GLUT1 K_m was 16.4±2.9 mM and the GLUT4 K_m was 6.85±1.5 mM.

$B_{max.}$ was 0.17±0.03 μM (from three experiments). The GLUT1 $B_{max.}$ for ATB-BMPA in chronically insulin-treated cells was 0.70±0.07 μM. The GLUT4 $B_{max.}$ in these cells was decreased to 0.099±0.017 μM (from three experiments).

A similar photolabel-displacement methodology was used to measure the separate affinity constants of GLUT1 and GLUT4 for 3-*O*-methyl-D-glucose. Concentrations of 3-*O*-methyl-D-glucose of 0–20 mM were incubated with the photolabel in either acutely or chronically insulin-treated 3T3-L1 cells. Fig. 6(*a*) shows that in acutely insulin-treated cells the K_m for 3-*O*-methyl-D-glucose displacement was 23.4±7.6 mM, which was ~ 3-fold higher than the GLUT4 K_m, which was 7.2±2.0 mM (from three experiments). In chronically insulin-treated cells (Fig. 6*b*) the GLUT1 K_m for 3-*O*-methyl-D-glucose was 16.4±2.9 mM and was ~ 3-fold higher than the GLUT4 K_m, which was 6.8±1.5 mM (from two experiments). The results of the 3-*O*-methyl-D-glucose displacement were used in conjunction with the $B_{max.}$ values to calculate TK values for GLUT1 and GLUT4 as described in the Discussion section. Table 1 shows that the TK value for GLUT4 was ~ 3-fold higher than for GLUT1.

In the basal state, the GLUT1 and GLUT4 K_m values for 3-*O*-methyl-D-glucose and their K_d values for the photolabel could not be examined directly by using the ATB-BMPA displacement methodology, because the radioactive ATB-BMPA incorporated was very low and any displacement by ligand would decrease the recovered radiolabel even further. However, we have shown, in basal rat adipocytes and 3T3-L1 cells, that the ATB-BMPA concentration required for half-maximal inhibition of transport is not significantly different from that required for half-maximal inhibition of transport in insulin-treated cells [21,23]. In view of the limited applicability of the photolabel-displacement methodology to the basal state, we have determined GLUT1 and GLUT4 levels from the photolabelling of basal cells with tracer concentrations (80 μM) of ATB-BMPA. We have then calculated the concentrations of unoccupied sites ($x1$ and $x4$ in eqn. 4 in the Discussion section), using the assumption that the K_d for ATB-BMPA and the K_m for 3-*O*-methyl-D-glucose were the same as in the insulin-stimulated cells. This analysis method (Table 1) showed that the calculated GLUT1 and GLUT4 TK values in basal cells were ~ 2-fold lower than in the insulin-treated cells. Because the analysis of photolabelling and transport data in the basal state involved greater error and used more assumptions than the analysis of the data from insulin-stimulated cells, we place less reliance on the TK values calculated for the basal cells.

DISCUSSION

Determination of the intrinsic activity of GLUT1 and GLUT4

We have shown that 80% of the cell-surface transporter labelling is immunoprecipitated by GLUT1 and GLUT4 antibodies. Thus if other isoforms are present they are not very abundant and are not likely to significantly contribute to transport. As discussed by Calderhead *et al.* [21], uptake is thus given by the sum of two Michaelis–Menten equations representing the separate flux attributable to each of the isoforms:

$$v = \frac{V_{max.1} \cdot S/K_{m1}}{(1+S/K_{m1})} + \frac{V_{max.4} \cdot S/K_{m4}}{(1+S/K_{m4})} \quad (1)$$

where $V_{max.}$ and K_m are the equilibrium exchange transport parameters.

$V_{max.}$ values are dependent on the transporter concentrations and the catalytic rate constants. The $1/(1+S/K_m)$ or $K_m/(K_m+S)$ terms represent the fraction of unoccupied sites. Thus eqn. (1) can be written as follows:

$$v = \frac{TK1 \cdot S \cdot [GLUT1]}{(1+S/K_{m1})} + \frac{TK4 \cdot S \cdot [GLUT4]}{(1+S/K_{m4})} \quad (2)$$

where [GLUT1] and [GLUT4] are the transporter isoform concentrations and TK1 and TK4 are the association constants, which are equal to turnover number/K_m and thus represent the tendency of the substrate to associate with unoccupied sites.

Values for the GLUT1 and GLUT4 concentrations used for substitution into eqn. (2) were determined from ATB-BMPA binding data, which we have shown in the Results section gave values for K_d and $B_{max.}$. The terms in eqn. (2) representing the reciprocal of the fraction of unoccupied sites can be directly obtained from the displacement of the photolabel, where:

$$A^0/A = 1+S/K_m \quad (3)$$

where A^0/A values are the ratios of the radioactivity associated with the photolabelled transporters in the presence (A) and absence (A^0) of competing 3-*O*-methyl-D-glucose and used to calculate the TK values shown in rows 1–3 in Table 1. The K_m values of GLUT1 and GLUT4 can also be obtained from the 3-*O*-methyl-D-glucose displacement of the photolabel (eqn. 3). These K_m values can then be used in an alternative method to calculate the fraction of unoccupied sites (rows 4–6 in Table 1).

Multiplying the $B_{max.}$ values by the fraction of unoccupied sites (either A/A^0 or $1/(1+S/K_m)$ gave $x1$ and $x4$ (the concentrations of unoccupied sites). Values of TK1 and TK4 were then derived from eqn. (4) by least-squares regression, by the methods described by Cleland [32]:

$$v/S = TK1 \cdot x1 + TK4 \cdot x4 \quad (4)$$

Table 1 compares the results of analysis of TK values carried out by several different methods for calculating the concentration of unoccupied sites. The method appears to be quite robust and can handle the combined errors involved in using transport data

Table 1. Calculation of GLUT1 and GLUT4 TK values for 3-*O*-methyl-D-glucose transport in 3T3-L1 cells

	Analysis method	$10^{-3} \times$ TK1 ($mM^{-1} \cdot min^{-1}$)	$10^{-3} \times$ TK4 ($mM^{-1} \cdot min^{-1}$)
1. Acute insulin	Direct use of A^0/A values $B_{max.1} = 0.19\ \mu M$ $B_{max.4} = 0.17\ \mu M$	4.90±2.03	7.92±2.86
2. Chronic insulin	Direct use of A^0/A values $B_{max.1} = 0.70\ \mu M$ $B_{max.4} = 0.099\ \mu M$	3.82±2.20	8.60±18.4
3. Combined data from acute and chronic treatments	Direct use of A^0/A values $B_{max.}$ values as above	3.71±0.31	9.50±1.26
4. Combined data from acute and chronic treatments	Acute insulin $K_{m1} = 23.4$ mM $K_{m4} = 7.2$ mM Chronic insulin $K_{m1} = 16.4$ mM $K_{m4} = 6.85$ mM $B_{max.}$ values as above	3.73±0.26	10.92±1.11
5. Combined data from acute and chronic treatments	Using average K_m: $K_{m1} = 19.9$ mM $K_{m4} = 7.0$ mM $B_{max.}$ values as above	3.58±0.24	11.34±1.06
6. Basal	Using average K_m: $K_{m1} = 19.9$ mM $K_{m4} = 7.0$ mM $B_{max.1} = 0.055\ \mu M$ $B_{max.4} = 0.015\ \mu M$	1.20±0.36	5.73±2.02

and A/A^0 values directly. TK values were obtained which were similar to those obtained when the error in $x1$ and $x4$ was decreased by using $x1$ and $x4$ values which were calculated from the 3-*O*-methyl-D-glucose K_m values. Table 1 shows that the TK values for GLUT1 and GLUT4 were similar for both the acute-insulin and the chronic-insulin treatments. The GLUT1 TK was found to be $0.36 \times 10^4\ mM^{-1} \cdot min^{-1}$, whereas the GLUT4 TK was ~3-fold higher ($1.13 \times 10^4\ mM^{-1} \cdot min^{-1}$). Multiplying these values by the GLUT1 and GLUT4 average K_m values of 20.0 and 7.0 mM respectively gave a GLUT1 turnover number, or catalytic rate constant, of $7.2 \times 10^4\ min^{-1}$ and a value for GLUT4 turnover number of $7.9 \times 10^4\ min^{-1}$. Thus, at low concentrations of 3-*O*-methyl-D-glucose, GLUT1 makes a substantially smaller contribution to flux than does an equal concentration of the GLUT4 isoform. However, this is due to the low affinity of GLUT1 for this substrate, which decreases its association with the transporter.

The GLUT1 turnover calculated from this data on 3T3-L1 cells ($7.2 \times 10^4\ min^{-1}$ at 37 °C) is of the same order as that calculated from GLUT1 in other systems, but at 20 °C. The GLUT1 turnover for 3-*O*-methyl-D-glucose at 20 °C has been determined in oocytes injected with GLUT1 mRNA [33,34]. Gould and Lienhard [33] estimated that their oocytes expressed 7 ng of GLUT1 per oocyte and calculated a turnover number of $1 \times 10^4\ min^{-1}$. However, Keller *et al.* [34] have estimated that their system expressed 0.2 ng of GLUT1 per oocyte and calculated a 3-*O*-methyl-D-glucose turnover at 20 °C of $13.4 \times 10^4\ min^{-1}$. Our own estimate of the rate constant for 50 μM-3-*O*-methyl-D-glucose uptake in erythrocytes at 20 °C was $15.2\ min^{-1}$ [35], giving a calculated turnover of $4.3 \times 10^4\ min^{-1}$ (assuming a GLUT1 concentration of 7 μM and a 3-*O*-methyl-D-glucose exchange K_m of 20.0 mM). The GLUT4 turnover that we have calculated from the data obtained for 3-*O*-methyl-D-glucose transport in 3T3-L1 cells ($7.9 \times 10^4\ min^{-1}$ at 37 °C) is very similar to that obtained in rat adipocytes, where the 3-*O*-methyl-D-glucose turnover at 37 °C was calculated by Simpson *et al.* [36] to be $5.6 \times 10^4\ min^{-1}$. Our own estimate [37] of the 3-*O*-methyl-D-glucose exchange $V_{max.}$ was $50.4\ mM \cdot min^{-1}$ at 37 °C. Since the GLUT4 concentration was ~1.5 μM (calculated from [36]), the calculated turnover number is $3.4 \times 10^4\ min^{-1}$.

In the basal state the calculated turnover numbers for GLUT1 and GLUT4 are ~2-fold lower than that found for insulin-stimulated 3T3-L1 cells. There are many inaccuracies in measuring transport and photolabelling in the basal state. However, the result is consistent with the ~1.5–2-fold suppression of transport activity in the basal state that we have shown in rat adipocytes [23,38].

Assumptions used in the analysis of GLUT1 and GLUT4 activity

In the analysis above, we have demonstrated that the ATB-BMPA displacement methodology can be used to provide information on the relative activities of the GLUT1 and GLUT4 transporters when these are present in the same cell population. The analysis assumes that the radioactivity recovered in the immunoprecipitates reflects the relative abundance of these isoforms, and we now examine this assumption.

We have attempted to determine whether all the sites which reversibly bind the photolabel irreversibly react with it when irradiated. We have shown from the transport inhibition observed at 0.5, 1 and 2 mM ligand that most of the sites bind label irreversibly when occupied. This would be consistent with observations made with human erythrocyte membranes, where close to 100% efficiency of the photochemical reaction was apparent with ATB-BMPA as the probe [26]. The high photochemical efficiency which is observed with the diazirine-substituted bis-hexose was much greater than that obtained with aryl azide-substituted compounds, where the estimated efficiency was only ~25% [39].

We have found that, after immunoprecipitation of both GLUT1 and GLUT4 from $C_{12}E_9$-solubilized cells, < 20% of the radioactivity running in the transporter region of the gel is left in

the immunoprecipitation supernatants. These findings are consistent with previous observations that the efficiencies of immunoprecipitation of GLUT1 and GLUT4 in human erythrocytes [26] and in rat adipocytes [23] are ~ 80%.

Another factor which is relevant to the use of ATB-BMPA to quantify the level of transporter isoforms is the affinity of the transporter for the ligand. In the present study we have observed that the K_i is ~ 250 μM in acutely and chronically insulin-treated cells. These results are similar to those in which transport inhibition by ATB-BMPA in erythrocytes showed a GLUT1 K_i ~ 250 μM [26]. Transport inhibition by ATB-BMPA in rat adipocytes (where GLUT4 is the predominant isoform) showed a GLUT4 K_i which was also ~ 250 μM [23]. A more direct way of examining the affinities of the two transporters for the ligand is to carry out photolabel-binding experiments at a range of concentrations. We have shown here that the affinity constants (in this case K_d) for ATB-BMPA binding to GLUT1 and GLUT4 are equal and are ~ 150 μM. The GLUT2 isoform in liver membranes also has a K_d for ATB-BMPA of ~ 200 μM (N. J. Jordan & G. D. Holman, unpublished work). Thus the binding of ATB-BMPA (a non-transported ligand) is approximately equal for all the mammalian isoforms tested (GLUT1, GLUT4 and GLUT2). However, these isoforms have different K_m values for transported substrates. The ability to bind a non-transported ligand at the outside site is kinetically a simpler reaction than that involved in binding and transporting a substrate. The apparent K_m for equilibrium sugar binding or exchange is dependent on rate constants for the membrane translocation step and the affinity constant at the inside site, and it is these parameters that may vary between different transporter isoforms.

These considerations suggest that the ATB-BMPA displacement methodology that we have used can be considered to give a good approximation of the transporter isoform concentrations at the cell-surface. We have shown that in acutely insulin-treated cells the GLUT1 concentration at the cell surface was 0.19 μM or 29.7 ng/35 mm dish, and the GLUT4 concentration was 0.17 μM or 27 ng/35 mm dish. This estimate of GLUT4 concentration compares reasonably well with the total cellular GLUT4 concentration as estimated by Western blotting. Calderhead *et al.* [21] found 50 ng/35 mm dish, and this is consistent with about half of GLUT4 being at the cells surface. However, the estimated cell surface GLUT1 appears to be a low proportion (~ $\frac{1}{5}$) of the total cellular GLUT1, which was determined by Western blotting to be 150 ng/35 mm dish [21].

We note that an under-estimate of the cell-surface glucose transporter concentration owing to factors such as low labelling or immunoprecipitation efficiency would lead us to over-estimate the transporter turnover numbers.

Regulation of the transport activities in 3T3-L1 cells

Large changes in cell-surface levels of glucose transporters occur in 3T3-L1 cells. We have determined that in basal cells the GLUT1:GLUT4 ratio was ~ 3:1. This was decreased by acute insulin treatment to 1:1, but increased to 10:1 owing to a prolonged chronic insulin treatment ([12]; the present work). It has been shown that in adipose cells translocation of GLUT4 glucose transporters from an intracellular pool [23,40–42] accounts for most of the observed acute insulin response. However, we have observed here that the intrinsic activities calculated from data obtained with insulin-stimulated cells cannot account entirely for the low transport rates observed in basal cells. This may be because the intrinsic activity of glucose transporters is slightly suppressed in the basal state, as suggested by Czech and co-workers [43,44] and by Zorzano *et al.* [45]. The analysis of intrinsic activity in the basal cells was not as accurate as that carried out with insulin-stimulated cells. However, GLUT1 and GLUT4 appear to have ~ 2-fold lower turnovers in basal cells. The suppression of GLUT1 activity may be slightly greater than suppression of GLUT4 activity.

The discrepancy between transport rate and photolabelling that we have observed here and elsewhere [21,38,46] suggest that the photolabel can combine with transporters that are at the surface but which do not participate fully in transport. We have suggested [46] that this suppression of transport activity may occur because transporters associate with trafficking proteins present as intermediates in the translocation process. An alternative possibility that has been suggested is that regulation of the activity of the GLUT1 isoform may be dependent on intracellular small molecules or inhibitory proteins which allosterically modify the transport catalysis rate [31,43,44,47]. This possible susceptibility of GLUT1 to allosteric control may account for the unusual kinetic properties of this isoform found in erythrocytes, where transport is kinetically asymmetric and shows accelerated exchange [28,47]. In contrast with these kinetic features of GLUT1 we have found [37] that in rat adipocytes, where GLUT4 is the predominant isoform and translocation is the predominant regulatory mechanism, the transport system is kinetically symmetric and does not show accelerated exchange.

Chronic insulin treatment greatly increases, by new protein synthesis, the total cellular content and the cell-surface concentration of GLUT1 [12,22], and we have suggested that this may be a response which compensates for the down-regulation of cell surface GLUT4 [12]. Consistent with this possibility is the observation that GLUT4 is down-regulated in 4–6 h, whereas GLUT1 rises steadily over 24 h. We have suggested [12] that the down-regulation of GLUT4 may be due to an impairment of the translocation mechanism, so that it may be of regulatory value to the cell to be able to produce, by new protein synthesis, an isoform which has different transport properties.

We are grateful to the M.R.C. and the British Diabetic Association for financial support.

REFERENCES

1. Pilch, P. F. (1990) Endocrinology (Baltimore) **126**, 3–5
2. Mueckler, M. (1990) Diabetes **39**, 6–10
3. Gould, G. W. & Bell, G. I. (1990) Trends Biochem. Sci. **15**, 18–22
4. Flier, J. S., Mueckler, M. M., Usher, P. & Lodish, H. F. (1987) Science **235**, 1492–1495
5. Birnbaum, M. J., Haspel, H. C. & Rosen, O. M. (1987) Science **235**, 1495–1498
6. Hiraki, Y., Rosen, O. M. & Birnbaum, M. J. (1988) J. Biol. Chem. **263**, 13655–13662
7. Rollins, B. J., Morrison, E. D., Usher, P. & Flier, J. S. (1988) J. Biol. Chem. **263**, 16523–16526
8. Cornelius, P., Marlowe, M., Lee, M. D. & Pekala, P. H. (1990) J. Biol. Chem. **265**, 20506–20516
9. Bird, T. A., Davies, A., Baldwin, S. A. & Saklatvala, J. (1990) J. Biol. Chem. **265**, 13578–13583
10. Haspel, H. C., Wilk, E. W., Birnbaum, M. J., Cushman, S. W. & Rosen, O. M. (1986) J. Biol. Chem. **261**, 6778–6789
11. Tordjman, K. M., Liengang, K. A. & Mueckler, M. (1990) Biochem. J. **271**, 201–207
12. Kozka, I. J., Clark, A. E. & Holman, G. D. (1991) J. Biol. Chem. **266**, 11726–11731
13. Thorens, B., Sarkar, H. K., Kaback, R. H. & Lodish, H. F. (1988) Cell **55**, 281–290
14. Kayano, T., Fukumoto, M., Eddy, R. L., Fan, Y.-S., Byers, M. G., Showa, T. G. & Bell, G. I. (1988) J. Biol. Chem. **263**, 15245–15248
15. James, D. E., Strube, M. I. & Mueckler, M. (1989) Nature (London) **338**, 83–87
16. Charron, M. J., Brosius, F. C., Alper, S. L. Lodish, H. F. (1989) Proc. Natl. Acad. Sci. U.S.A. **86**, 2535–2539
17. Kaestner, K. H., Christy, R. J., McLenithan, J. C., Braiterman, L. T., Cornelius, P., Pekela, P. H. & Lane, M. D. (1989) Proc. Natl. Acad. Sci. U.S.A. **86**, 3150–3154

18. Birnbaum, M. J. (1989) Cell **57**, 305–315
19. Fukumoto, H., Kayano, T., Buse, J. B., Edwards, Y., Pilch, P. F., Bell, G. I. & Seino, S. (1989) J. Biol. Chem. **264**, 7776–7779
20. Kayano, T., Burant, C. F., Fukumoto, H., Gould, G. W., Fan. Y.-S., Eddy, R. L., Byers, M. G., Shows, T. B., Seino, S. & Bell, G. I. (1990) J. Biol. Chem. **265**, 13276–13282
21. Calderhead, D. M., Kitagawa, W., Tanner, L. T., Holman, G. D. & Lienhard, G. E. (1990) J. Biol. Chem. **265**, 13800–13808
22. Tordjman, K. M., Leingang, K. A., James, D. E. & Mueckler, M. (1989) Proc. Natl. Acad. Sci. U.S.A. **86**, 7761–7765
23. Holman, G. D., Kozka, I. J., Clark, A. E., Flower, C. J., Saltis, J., Habberfield, A. D., Simpson, I. A. & Cushman, S. W. (1990) J. Biol. Chem. **265**, 18172–18179
24. Stein, W. D. (1986) Transport and Diffusion across Cell Membranes, pp. 356–357, Academic Press, London
25. Holman, G. D. & Midgley, P. J. W. (1985) Carbohydr. Res. **135**, 337–341
26. Clark, A. E. & Holman, G. D. (1990) Biochem. J. **269**, 615–622
27. Frost, S. C. & Lane, M. D. (1985) J. Biol. Chem. **260**, 2646–2652
28. Eilam, Y. & Stein, W. D. (1972) Biochim. Biophys. Acta **266**, 161–173
29. Rees, W. D. & Holman, G. D. (1982) Biochim. Biophys. Acta **642**, 251–260
30. Deves, R. & Krupka, R. M. (1984) Biochim. Biophys. Acta **769**, 455–460
31. Clancy, B. M., Harrison, S. A., Buxton, J. M. & Czech, M. P. (1991) J. Biol. Chem. **266**, 10122–10130
32. Cleland, W. W. (1979) Methods Enzymol. **63**, 103–138
33. Gould, G. W. & Lienhard, G. E. (1989) Biochemistry **28**, 9447–9452
34. Keller, K., Strube, M & Mueckler, M. (1989) J. Biol. Chem. **264**, 18884–18889
35. Holman, G. D., Busza, A. L., Pierce, E. J. & Rees, W. D. (1981) Biochim. Biophys. Acta **649**, 503–514
36. Simpson, I. A., Yver, D. R., Hissin, P. J., Wardzala, L. J., Karnieli, E., Salans, L. B. & Cushman, S. W. (1983) Biochim. Biophys. Acta **763**, 393–407
37. Taylor, L. P. & Holman, G. D. (1980) Biochim. Biophys. Acta **642**, 325–335
38. Clark, A. E., Holman, G. D. & Kozka, I. J. (1991) Biochem. J. **278**, 235–241
39. Holman, G. D., Parkar, B. A. & Midgley, P. J. W. (1986) Biochim. Biophys. Acta **855**, 115–126
40. Cushman, S. W. & Wardzala, L. T. (1990) J. Biol. Chem. **255**, 4758–4762
41. Suzuki, K. & Kono, T. (1980) Proc. Natl. Acad. Sci. U.S.A. **77**, 2542–2545
42. Slot, J. W., Gueze, H. J., Gigengack, S., Lienhard, G. E. & James, D. E. (1991) J. Cell Biol. **113**, 123–135
43. Clancy, B. M. & Czech, M. P. (1990) J. Biol. Chem. **265**, 12434–12443
44. Harrison, S. A., Buxton, J. M., Clancy, B. M. & Czech, M. P. (1990) J. Biol. Chem. **265**, 20106–20116
45. Zorzano, A., Wilkinson, W., Kotliar, N., Thoidis, G., Wadzinski, B. E., Ruoho, A. E. & Pilch, P. F. (1988) J. Biol. Chem. **264**, 12358–12363
46. Yang, J., Clark, A. E., Harrison, R., Kozka, I. J. & Holman, G. D. (1992) Biochem. J. **281**, 809–817
47. Carruthers, A. (1990) Physiol. Rev. **70**, 1135–1176

Received 3 September 1991/2 December 1991; accepted 13 December 1991